New High-Power Controlled Source Electromagnetic System for Geothermal Applications

Yardenia Martinez[1], Abdul Latif Ashadi[2], Hector R. Hinojosa[1,3], Pantelis Soupios[2], and Kurt Strack[1]

[1]KMS Technologies, USA,
[2]King Fahd University of Petroleum & Minerals, Saudi Arabia,
[3]Cordillera Geo-Services LLC, USA

Keywords

Controlled-source electromagnetics (CSEM), magnetotellurics (MT), electrical anisotropy, geothermal exploration, monitoring

ABSTRACT

Electromagnetic (EM) methods have been widely used in geothermal exploration. EM passive methods such as Magnetotellurics (MT) and Audio Magnetotellurics (AMT) have been the industry standard due to the existing 3D interpretation tools.

Passive methods encounter a few problems, including variations in signal strength, azimuth, static shift, and others stemming from cultural noise. A new high-power controlled-source electromagnetics (CSEM) array system offers a solution to these issues. By combining passive MT/AMT, CSEM measurements, and Cloud-enabled EM data acquisition and quality control, the EM array system provides a better solution in areas of high cultural noise and real-time quality checks of field data. We clearly see this in the field data examples.

As we enter the energy transition, geothermal production with CO_2 injection or cooling and re-injection of the produced fluid are of great interest for development and investment. By acquiring passive MT/AMT and CSEM, we obtain complementary measurements from both applications for exploration and monitoring.

1. Introduction

Hydrothermal exploration typically uses electromagnetic methods. Calibration of these methods against drilling results has been done in several geothermal fields, and resistivity measurements can be used as a subsurface thermometer (Christensen et al., 2004). The correlation between resistivity and temperature is associated with the degree of hydrothermal alteration (Noor et al., 2012). The higher temperatures and salinity of the pore water and increased rock alteration associated with geothermal areas often decrease the bulk resistivity in a rock mass, ideal for detection using passive MT/AMT. The bulk resistivity is further lowered if faults and fracture zones cross-cut the geothermal play (Moeck, 2014).

Passive MT and AMT use solar activity interacting with the Earth's magnetic field and thunderstorms as their electromagnetic signal source. Because of this, the signal has variable strength and azimuth of the primary field, which are often time-dependent. Also, in periods of low solar activity, the weak source signal is overrun in high cultural noise areas, making it difficult to acquire high-quality data in a reasonable time without extending recording times to several days, which might or might not help. Nowadays, it is more difficult to find areas of exploration free of human activity. In addition, MT and AMT also suffer from static shifts caused by sharp lateral variations in the near-surface electrical conductivity (Cummings and Maechie, 2010; Strack, 1992).

As CSEM is an active method that uses an artificial energy source, this method overcomes the challenges faced by passive MT/AMT. Two main advantages of the CSEM method over the passive MT/AMT are: complete control over the strength and waveform of the source signal and the possibility to tailor the source signal based on the area's noise level. Furthermore, the CSEM source signal can be transmitted in multiple directions, providing additional information regarding the electrical anisotropy of the under-laying sediments. These factors allow for a higher signal-to-noise-ratio (SNR), providing a higher resolution of the reservoirs of interest which can also be used for monitoring applications. Figure 1 shows an illustration of the difference in resolution between the methods.

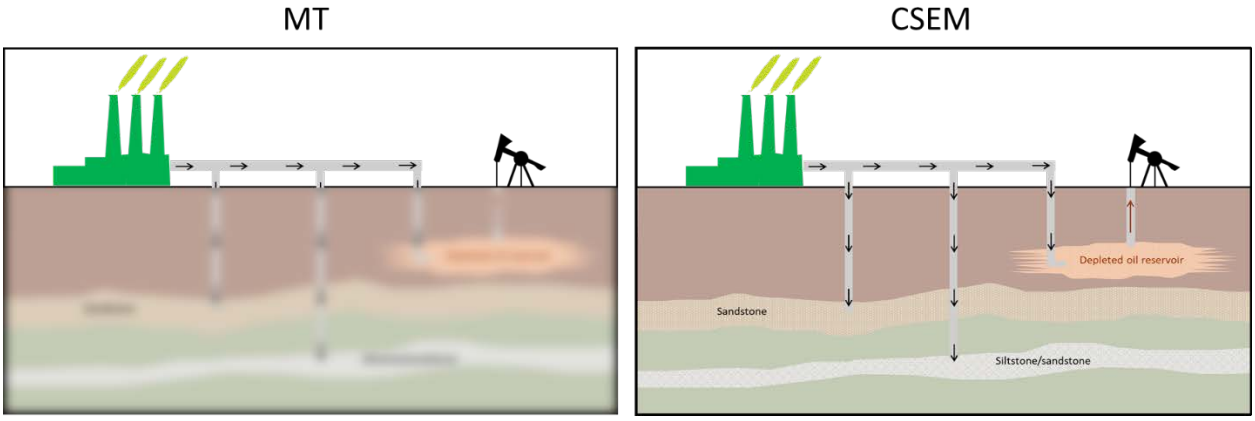

Figure 1: Illustration of the expected resolution for MT (left) and CSEM (right). In general, MT provides the subsurface resistivity distribution. However, it struggles at providing a clear image of the layers' interfaces as well as their lateral distribution. On the other hand, CSEM records stronger EM responses due to the active source, thus providing better resolution of the subsurface which yields to more accurate geologic interpretations.

EM measurements are not only valuable for the exploration stage of any style of geothermal plays worldwide, but can also assist in monitoring the fluid injection in a geothermal producing field and CO_2 injection. Next, we discuss some of the differences between CSEM and MT/AMT methods for mapping buried structural features (faults and fracture zones) and locating heat sources. The equipment used to record the EM signal in a CSEM survey is the same as MT, but

the energy source is a high-power transmitter shown in Figure 2 (instead of natural EM plane waves used in MT).

Figure 2: Left: CSEM high-power transmitter, up to 400 Amps reversing (KMS-150). Right: EM receivers (KMS-820 array system). The same receivers are used to record MT/AMT and/or CSEM.

2. CSEM survey configuration

In a CSEM survey, the source signal is injected into the ground via a horizontal electric dipole, typically 1 km long. The dipole source transmits a carefully designed electromagnetic signal, which is recorded by an array of electric and magnetic field receivers located at various distances from the energy source. The receivers can be deployed either in a 2D or 3D configuration. Figure 3 shows an example of the typical CSEM hardware configuration (Strack et al., 1990; Strack, 1992). The received signal is a function of the input current, which is modified by the resistivity structure of the Earth between the transmitter and receiver(s) and by the acquisition system itself; superimposed on this response are various sources of anthropogenic and natural noise (Strack, 1992; Haroon et al., 2020). In high noise areas, the SNR is enhanced by increasing the source dipole moment (current and dipole length) and increasing recording times. CSEM recording times range from 2 to 6 hours and depend on the depth of investigation, average resistivity of the subsurface layers, and overall noise level. Conversely, MT and AMT can require over 24 hours in high cultural noise areas without guaranteeing that the recorded data are of sufficient quality for further processing. Figure 4 shows an example that compares MT and CSEM data for receivers in a high noise area within 1 km from an electric power plant and receivers away from it (> 1 km). For the MT data, the apparent resistivities of the receiver located within the high noise area, show high uncertainty and unclear distributions. For the CSEM, receivers inside the high-noise area shows similar signal signature to the one located in a low-noise area (as longer recording time allow improving S/N ratios). This translates itself to comparative interpretation quality shown below for the data examples.

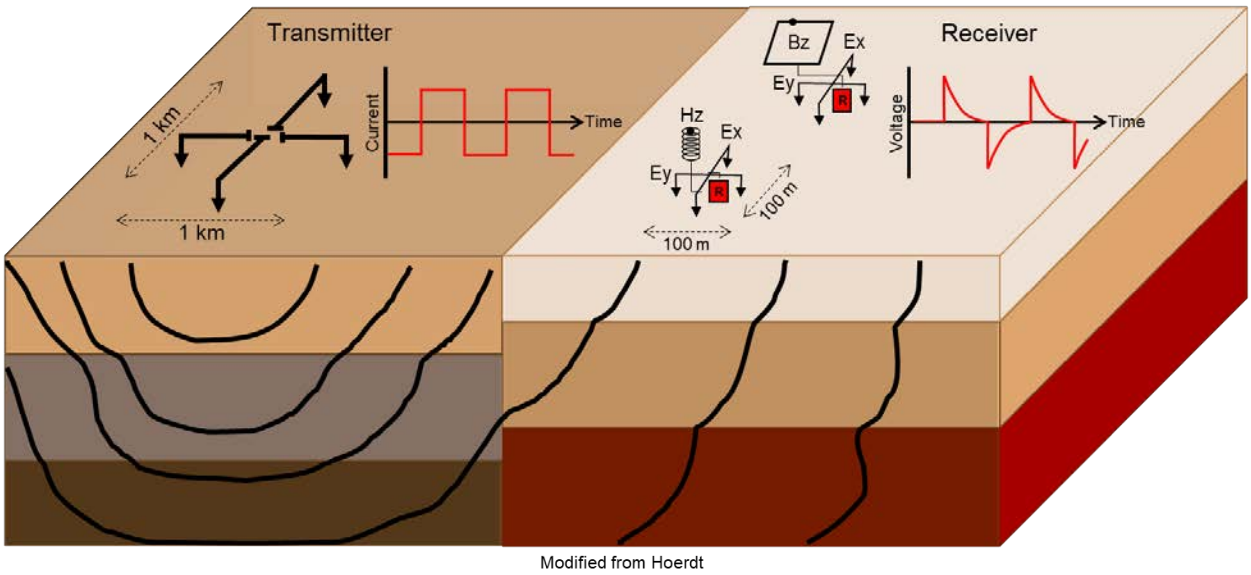

Figure 3: Example of a CSEM survey setup depicting a transmitter on the left and various receivers on the right. The transmitter waveform shown is a square wave (on the left) and the corresponding receiver signals are transients (on the right). The contour lines over the cross section represents lines of equal current density for different times after switching.

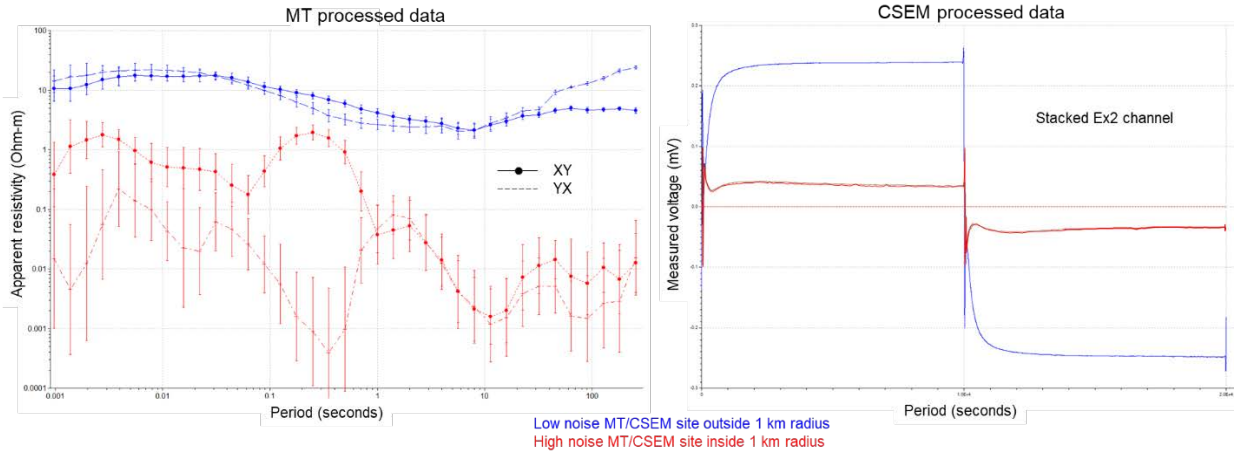

Figure 4: MT and CSEM data processing results of a site inside the 1 km radius of a power plant (noisy site) and a site outside the 1 km radius (low noise site). Left: MT apparent resistivity curves for the XY and YX components, right: CSEM stacked data for Ex2 channel for one period. The red curves represent data from a site near the power plant. The blue curves depict data from a site away from the plant in a low noise area (site map is in Fugure 5).

Another essential difference between CSEM and passive MT/AMT is that the latter is based on the simultaneous measurement of 5 electromagnetic field components (3 magnetic fields H and 2 electric fields E). The electrical conductivity of the underlying material is determined by the ratio of the measured electric (E) and magnetic field (H) variations, or MT transfer functions: the horizontal electric (Ex and Ey) and horizontal magnetic (Hx and Hy) (Naidu, 2012). In CSEM, the electrical conductivity from the subsurface can be estimated from any of the measured field components alone.

Apart from noise, a complex subsurface geologic structure can introduce 3D effects to the recorded data and is usually seen in the vertical magnetic field Hz. Electric anisotropy resulting from stratigraphic variations is more challenging to account for with traditional MT/AMT measurements because they are biased towards conductive strata. However, CSEM measurements – as they are sensitive to conductive and resistive strata, can be designed to effectively detect electrical anisotropy. For instance, the signal is transmitted by two horizontal electrical dipoles oriented in perpendicular directions. The two transmitting dipoles can be deployed (in a T or L shape). After the transmitting and recording is completed for one direction, the transmitting direction changes and is recording repeats. Specifically, this setup allows to observe differences in the recorded signals and determine if electrical anisotropy during the near real time quality assurance. Understanding electrical anisotropy is crucial for properly monitoring and interpreting fluid movement and detecting compromised seals where leakage can occur. It can also aid in efficiently targeting and drilling conduction-dominated geothermal play systems (i.e., petrothermal reservoirs), which have become highly interesting and economically viable in recent years.

3. CSEM data examples

We show two recent examples, one from a monitoring application in the US and one from a geothermal feasibility survey in Saudi Arabia both acquired with the same system. In early spring 2021, MT and CSEM baseline surveys were acquired in Northern US as part of a monitoring project for carbon capture and storage (CCS), Figure 5 shows the configuration for both the MT and CSEM measurements, the top left shows the MT site setup, to the right is the full survey configuration, MT sites were deployed every 600 m while CSEM sites were deployed every 200 m, bottom images show the CSEM site setup, on the left is the typical transmitter setup, a total of two transmitter locations were used, to the right is the hardware configuration for CSEM. Before the acquisition, a 3D Feasibility was carried out to estimate the CSEM response before and after CO_2 injection. The goal is to optimize acquisition parameters and to determine if signals could be detected in the field in the presence of the observed noise levels (measured during the Feasibility).

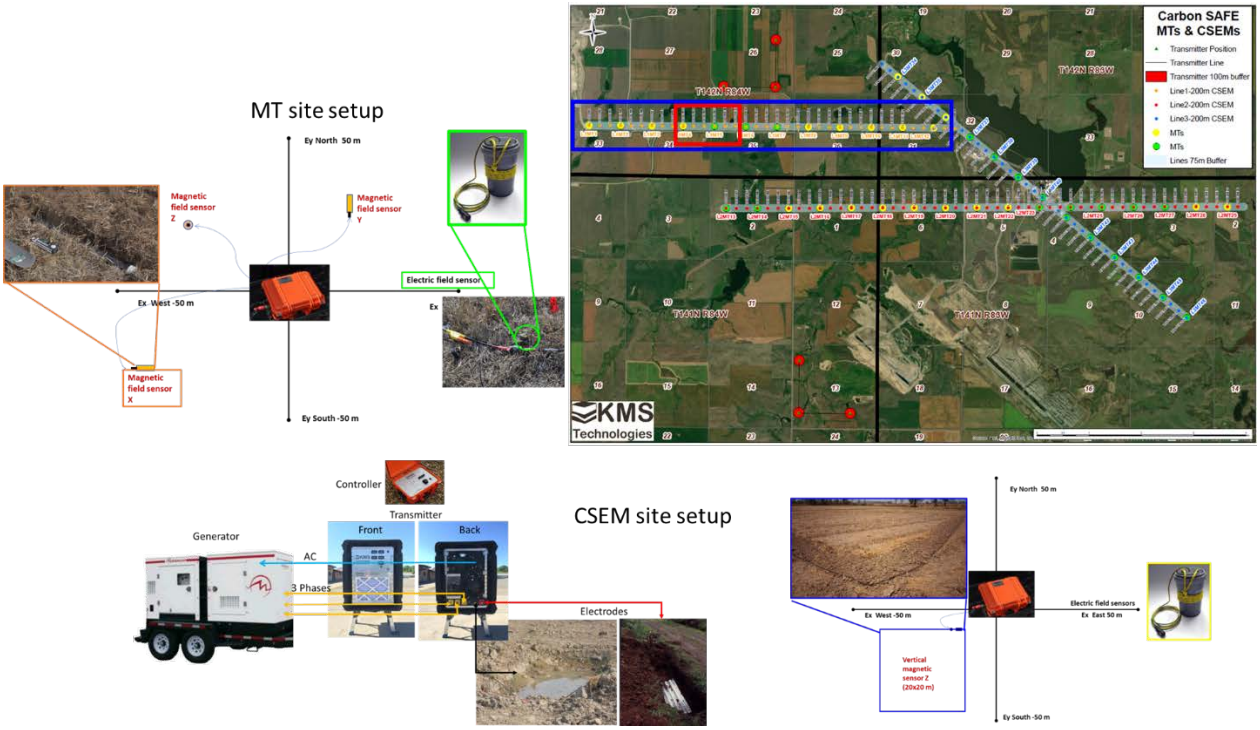

Figure 5: MT and CSEM survey configuration. Both MT & CSEM sites were acquired along lines where seismic had already been acquired. Top left is a schematic of the MT site setup, horizontal electric fields were measured with dipoles 50 m long, with non-polarized, lead free electrodes, magnetic fields were measured in two horizontal directions and one vertical using wide-band induction coil magnetometers. In the top right is the study area survey configuration, MT sites are depicted as yellow and green dots 600 m apart, CSEM sites were deployed every 200 m (overlapping MT sites every third), CSEM sites are represented with the smaller orange, red and blue dots. At the bottom left are pictures illustrating the transmitter setup for a single dipole direction, to the right is the CSEM site setup, horizontal electric fields are measure just as MT, however, the vertical magnetic field is measured using a coil loop cable. The blue square outlines the sites for the MT and the red the ones for the CSEM data shown in the following figure.

The feasibility study results indicate that the injection of CO_2 over at least 18 months will provide a sufficiently different EM response to detect and interpret the fluid change. Also, the 3D feasibility modeling provides an optimized survey design with adequate hardware selection to minimize noise effects on the data.

Cloud-enable data acquisition was part of this survey and was fundamental to ensure high-quality data being recorded and efficiently acquire the survey minimizing the number of hardware pickups and re-deployments. Real-time quality checks allow for remote site processing of MT and CSEM data, which translates into making decisions on whether to leave stations to record for longer time. For CSEM, these quality checks resulted in onsite optimization of the transmitted waveform. Offsite processing provides evidence that all near-time decisions made during data acquisition resulted in a dataset where most of the data is rated as excellent and/or good, ideal for further interpretation. The ultimate data quality proof is in match of the inversions and a 3D data-driven model to borehole scale. Both showing strong agreement with existing seismic interpretation (structure) and nearby wells (resistivity distribution from logs). Figure 6 shows the results of the MT and CSEM field data after processing and inversion. On top is the 2D MT inversion results along one of the acquired lines. The recorded sites are marked as black triangles, the profile shows the variations in resistivity where structure of the layers is recovered, the red rectangle shows the

coverage of the CSEM profile shown below. In the CSEM profile, on the left are the unsupervised 1D inversion results compared with the borehole log. There is a good match between them and is is obvious that the MT has less sensitivity to the resistivity structure than the CSEM. However, the MT see the overall picture and resistivity background much better than the CSEM. On the right of the figure is the 3D model-based CSEM data compared with the field CSEM data at one site. The reservoir response times (this is time domain CSEM) where CO_2 injection will occur is depicted with the dark brown rectangle. The 3D modeled data matches all components within that time window, Ex-components are noise dominated at late time as for the site configurartion they are perpendicular to the transmitter dipole, thus the signal can be neglected. Overall, these results are an excellent validation of the data information content, and we expect that we will naturally see and match the CO_2 fluid injection anomaly in future repeat measurements.

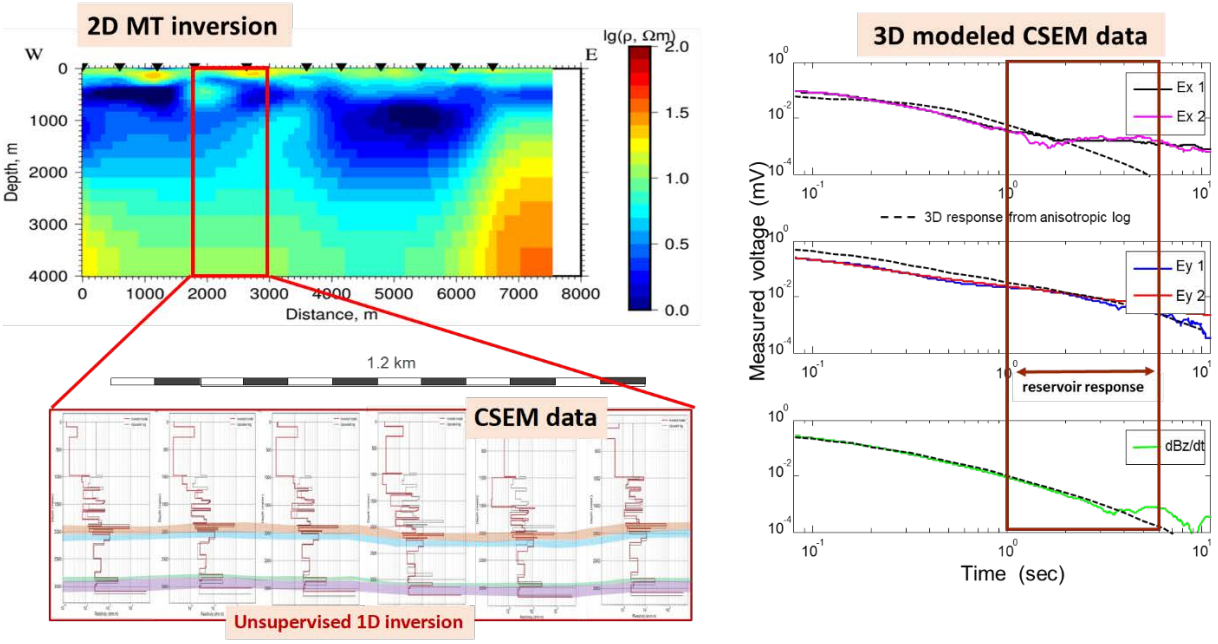

Figure 6: MT & CSEM data examples. Top 2D MT inversion results along one of the acquired line, MT sites are depicted with the black triangles, the results show a conductor (in blue) with variable thickness along the profile, thus suggesting some structure of the layering. The dark red rectangle markes the profile covered by CSEM below. In the CSEM data example; left: a short profile showing the inversion results in red and borehole log in black, the orange, blue, green and violet lines along the profile highlight different geologic formations. Right: the various EM components (colored curves) compared to the 3D model (borehole log) response. The dark brown box shows the time interval where we expect the reservoir responses. Where the colored curves deviate at later times from the 3D response (black dashed lines), the signal disappears in the noise.

The successful acquisition of this survey is twofold. First, it highlights the capability of CSEM in areas with anthropogenic activity and high noise for applications such as monitoring where high resolution is needed. Second, it verifies the assumptions made during the 3D feasibility were correct; where the measurements are able to image the reservoir levels of interest BEFORE actually carrying out the time-lapse survey.

Borehole electric measurements helped us better understand electrical anisotropy in the study area. From the MT and CSEM data acquired, we found little evidence in the MT data of the so-called "3D effects" (usually related to the structure or electrical anisotropy imposed by bedding planes). Likewise, the recorded CSEM data shows slight variations between different transmitter orientations, suggesting minimal geologic structure and where the layering appears isotropic. This was further confirmed by seismic sections provided for this project. We do see static effects in both the MT and CSEM data and correct for them appropriately (by calibration or including in 3D models) as they are outside of the signal window of interest

Another example is from a recent field test in Saudi Arabia. A test survey line was done within the vicinity of a hot spring to evaluate the subsurface distribution of the heat source. Figure 7 shows the composite results of the MT. Other methods were applied (gravity, aeromagnetics, seismic etc.) and in the near future CSEM survey and more extended MT surveys will be carried out. The data was transmitted to the Cloud and the interpretation was done within 1 week of survey completion by a newly trained team of geophysicists. On the left of Figure 7, the resistivity section shows a low resistivity (red) zone which is most likely the heat source. The medium resistivity appears to be the conduit of hot water under the volcanics. The break in the volcanics and rising of hot fluid is visible to the left side of the hot springs. This gives further drilling targets to the left of the Hot Springs indicated in the figure.

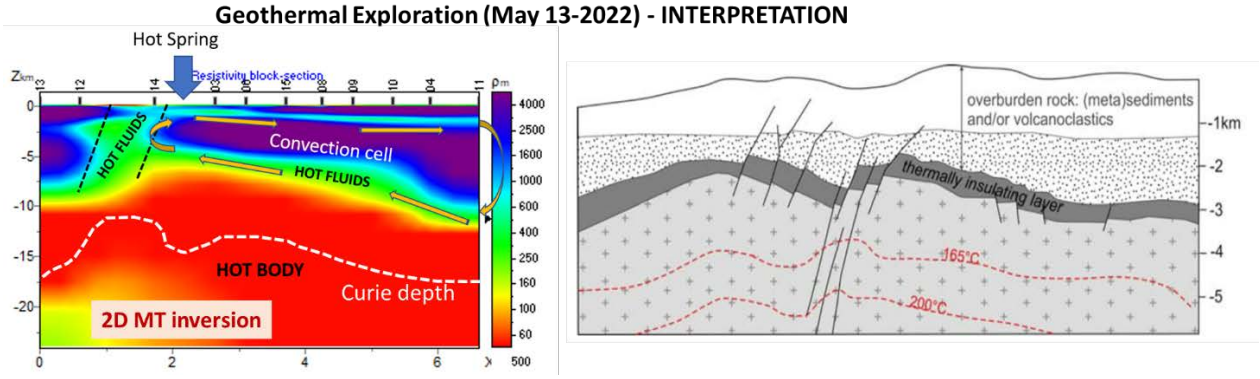

Figure 7. Example of geothermal exploration in Saudi Arabia. Left: 2D MT inversion results, on the right is a geologic cross-section overlaid with different temperature interpretations (after Soupios et al., 2022 and International Geothermal Association, 2014 - right section).

4. Conclusion

Electromagnetics remains among the best geophysical methods for mapping fluid changes, which make them ideal for geothermal exploration and monitoring producing fields. By showing the results of CSEM and MT survey acquisition near a coal power plant for a CO_2 injection project, we demonstrate the advantages of utilizing a high-power array CSEM system in areas with high cultural noise. CSEM has proven to be a great tool for providing information on the electrical anisotropy of the overburden, this was confirmed through the 1D inversion and 3D model-based data, as both use anisotropic models that resulted in a good match between modeled and field data. Ultimately, the workflows followed **3D Feasibility** for generating optimized survey configurations, coupled with **cloud-based real time quality control assurance** during the **acquisition**, proofs at all steps that the measurements are close to expectations, which further provides confidence and reduces the risk. During monitoring of a reservoir, we expect similar

changes in response than those estimated during the 3D Feasibility. CSEM surveys are suitable for most types of geothermal play. We experience the same quality results in a subsequent survey in Saudi Arabia motivating for further work in the coming years. Indeed, the geological understanding of a geothermal play, and its use, help to adopt site-specific exploration and field deployment of CSEM technologies.

Acknowledgments

The authors would like to thank our colleagues at KMS Technologies & KFUPM for contributing to this paper. We thank the financial supporters. The work in North Dakota was funded by DOE NETL as part of Cooperative Agreement DE-FE0031889 and supported by the EERC of the University of North Dakota and Minnkota Power Cooperative. The work in Saudi Arabia was funded by KFUPM.

REFERENCES

Christensen, P. R., Jakosky, B. M., Kieffer, H. H., Malin, M. C., McSweene Jr., H. Y., Nealson, K., Mehall, G. L., Silverman, S. H., Ferry, S., Caplinger, M. and Ravine, M. "The thermal Emission Imaging System (THEMIS) for the Mars 2001 Odyssey Mission." *Space Science Reviews* 110 (2004), 85-130. https://doi.org/10.1023/B:SPAC.0000021008.16305.94

Cummings, W., and Mackie, R. "Resistivity Imaging of Geothermal Resources Using 1D, 3D, and 3D MT Inversion and TDEM Static Shift Correction Illustrated by a Glass Mountain Case History", *Proc. World Geothermal Congress,* Bali, Indonesia, (2010)

Haroon, A., Swidinsky, A., Hölz, S., Jegen, M., and Tezkan, B. "Step-on versus step-off signals in time-domain controlled-source electromagnetic methods using a grounded electric dipole." *Geophysical Prospecting*, 68, (2020), 2825-2844.

International Geothermal Association (IGA). "Best Practices Guide for Geothermal Exploration" , IGA & IFC (International Finance Corporation) (2014),196 pp.

Moeck, I. S. "Catalog of geothermal play types based on geologic controls." *Renewable and Sustainable Energy Reviews*, 37 (2014), 867-882,

Naidu, G. D. "Magnetotellurics: Basic Theoretical Concepts in Deep Crustal Structure of the Son-Narmada-Tapti Lineament, Central India." *Springer*, Berlin, Heidelberg (2012), 13-35.

Noor, Y., Suwai, J., and Kangogo D. "Correlating Resistivity With Temperature and Alteration Mineralogy in Menengai Geothermal Field: Case Study of Menengai Exploration Well (MW-01)." *GRC Transactions*, 36 (2012), 731-736.

Soupios, P., Al-Karnos, A., Al Saibani, A., Ashadi, A. L., Hanstein, T., Khogali, A., Kirmizakis, P., Martinez, Y., Paembonan, A., Strack, K., and Xu, X. "High power CSEM and MT/AMT field test in Saudi Arabia – Geothermal Exploration." *Center of Integrated Petroleum Research-CIPR, College of Petroleum Engineering and Geosciences-CPG, Geophysics Program* (2022).

Stack, K. M. "Long-offset transient electromagnetic (LOTEM) depth soundings applied to crustal studies in the Black Forest and Swabian Alb, Federal Republic of Germany." *Geophysics*, 55(7), (1990), 834-842.

Strack, K. M. "Exploration with Deep Transient Electromagnetics." *Elsevier*, (1992), 373 pp.